

Ferrimagnets with a ‘weak’ magnetic sublattice

K P Belov

Contents

1. Introduction	623
2. ‘Weak’ magnetic sublattice in ferrimagnets with a magnetic compensation point	623
3. Low-temperature paraprocess and ‘low-temperature point’ T_B in a ‘weak’ sublattice	626
4. ‘Weak’ sublattice in ferrimagnets with an anomalous temperature behaviour of the spontaneous magnetization (Néel’s M and P curves)	629
5. ‘Weak’ sublattice in magnetite. On the low-temperature transformation problem ($T_t = 100 - 120$ K)	632
6. Conclusions	633
References	633

Abstract. Measurements on the anomalous temperature behaviour of the spontaneous magnetization in various ferrimagnets (N -, M -, and P -type Néel curves) are analyzed and summarised. The concept of a ‘weak’ magnetic sublattice is applied to explain the anomalies as well as manifestations of the ‘low-temperature point’ T_B and the antiferromagnetic-type paraprocess. The paraprocess phenomenon causes sign anomalies in the magnetocaloric effect, magnetostriction, and the ‘first’ component of the isotropic magnetoresistance. It is suggested that in magnetite (Fe_3O_4) the role of a ‘weak’ sublattice is played by the spin-ordered subsystem of hopping electrons (‘magneto-electron’ sublattice), and the appearing point T_B is nothing else but the low-temperature transformation point T_t (100–120 K).

1. Introduction

The theoretical study of ferrimagnets was pioneered by Néel in his seminal 1948 paper [1] on spinel ferrite as a prototype. The same paper introduces the term ‘ferrimagnetism’ for substances possessing noncompensated antiferromagnetism.

Ferrimagnets constitute a large group of magnetic materials, many of which have technological applications. Along with the spinel ferrites, they also include iron garnets, hexaferrites, rare-earth–iron intermetallic compounds, and some other substances.

One of the major predictions of Néel’s theory is that, depending on the temperature behaviour of the spontaneous magnetization, $I_s(T)$, ferrimagnets can be divided into two groups.

In one, ferrimagnets have the same Weiss-type $I_s(T)$ dependence found in ordinary ferromagnets [$I_s(T)$ curves of Q -type in the Néel’s notation].

The second group includes ferrimagnets showing anomalous $I_s(T)$ variation, namely ones with a magnetic compensation point Θ_c (N -type curves) or those exhibiting a low-temperature anomaly in that, as T increases, I_s grows instead of decreasing (M - and P -type curves).

In the early 60s, based on the temperature dependence of the spontaneous magnetization of gadolinium iron garnet $\text{Gd}_3\text{Fe}_5\text{O}_{12}$, the present author [2, 3] suggested that the appearance of the point Θ_c in this particular ferrite is due to a ‘weakly ordered’ (i.e. subject to a weak exchange field) gadolinium sublattice, which was later named ‘weak’ [4]. As further research has shown, this sublattice also accounts for the appearance, in $\text{Gd}_3\text{Fe}_5\text{O}_{12}$, of the so-called ‘low-temperature point’ T_B ,† as well as explaining the ferromagnetic- and antiferromagnetic-type low-temperature paraprocess and some concomitant effects.

The present review is aimed at extending the notion of a ‘weak’ sublattice to other ferrimagnets with anomalous $I_s(T)$ dependence (N -, M -, and P -type curves in Néel’s notation), in order to explain the magnetic, magnetostriction, thermal, electric, and other anomalies occurring in them.

2. ‘Weak’ sublattice in ferrimagnets with a magnetic compensation point

Table 1 lists the ferrimagnets with a Θ_c point, known to date. They include iron garnets of heavy rare-earth metals, some rare-earth–iron(cobalt) intermetallic compounds, spinel ferrites doped by Li, Cr, V, Al cations, and intermetallic Mn_5Ge_2 compound.

From general arguments, an anomalous — in particular, a Θ_c -point containing — temperature dependence of the spontaneous magnetization $I_s(T)$ of a ferrimagnet clearly implies a significant difference between its sublattice $I_s(T)$ curves.

A comparative analysis has been made [2, 3] on the $I_s(T)$ curves of the ferrites $\text{Gd}_3\text{Fe}_5\text{O}_{12}$, which has a Θ_c point, and $\text{Y}_3\text{Fe}_5\text{O}_{12}$, with a Weiss-type $I_s(T)$ curve. Since the Y^{3+} cation is nonmagnetic, the $I_s(T)$ curve in $\text{Y}_3\text{Fe}_5\text{O}_{12}$ may be thought

K P Belov M V Lomonosov Moscow State University,
Physics Department,
Vorob’evy Gory, 119899 Moscow, Russia
Tel. (7-095) 939 30 39, 939 20 03

Received 30 October 1995
Uspekhi Fizicheskikh Nauk 166 (6) 669–681 (1996)
Translated by E G Strel’chenko; edited by A Radzig

† The author designated this point as T_l with a subscript l (low) in his early publications. Here T_B is introduced instead of T_l .

Table 1. Ferrimagnets possessing a magnetic compensation point Θ_c and ‘low-temperature point’ T_B

Ferrimagnet	Θ_c , K	Ref.	T_B , K	Ref.	T_C , K*
Gd ₃ Fe ₅ O ₁₂	295	[5]	70–100	[5–7]	556
Tb ₃ Fe ₅ O ₁₂	250	[5]	58	[7]	553
Dy ₃ Fe ₅ O ₁₂	220	[5]	42	[7]	552
Ho ₃ Fe ₅ O ₁₂	130	[5]	32	[7]	548
Er ₃ Fe ₅ O ₁₂	85	[5]	20	[7]	547
GdFe ₃	615	[8]	—	—	725
TbFe ₃	595	[8]	—	—	655
DyFe ₃	545	[8]	—	—	605
HoFe ₃	395	[8]	170	[9]	570
ErFe ₃	250	[8]	—	—	555
HoFe ₂	240	[8]	—	—	594
ErFe ₂	210	[10]	—	—	576
DyCo _{5.2}	140	[11, 12]	—	—	~1000
TbCo _{5.1}	130	[11]	—	—	~1000
(Gd ₁₅ Co ₈₅) _{0.86} Mo _{0.14}	220	[13]	—	—	400
Li _{0.5} Fe _{0.9} Cr _{1.6} O ₄	283	[14]	—	—	440
Li _{0.5} Fe _{1.25} Cr _{1.25} O ₄	320	[15]	102	[15]	500
NiFe _{1.33} V _{0.67} O ₄	300	[16]	—	—	670
NiFe _{1.1} Cr _{0.9} O ₄	395	[16]	—	—	600
Mn ₅ Ge ₂	400	[18]	113	[17]	670

* For most of the tabulated substances, the temperature values are determined by the Belov–Goryaga–Arrot method, which yields more accurate T_C ’s than those obtained by drawing a tangent to the steepest portion of the $I_s(T)$ curve.

to give the temperature dependence of the spontaneous magnetization for the ‘united’ *ad*-sublattice of Gd₃Fe₅O₁₂. Such ‘replacement’ of *ad* sublattices is justified by the fact that both ferrites have practically the same Curie temperatures ($T_C = 556$ K and 551 K for Gd₃Fe₅O₁₂ and Y₃Fe₅O₁₂, respectively) and hence the same parameters of the intersublattice *ad*-exchange interactions. Also, crystallographical studies have shown that the geometrical arrangement of the Fe³⁺ cations in rare-earth–iron garnets is nearly the same as in Y₃Fe₅O₁₂.

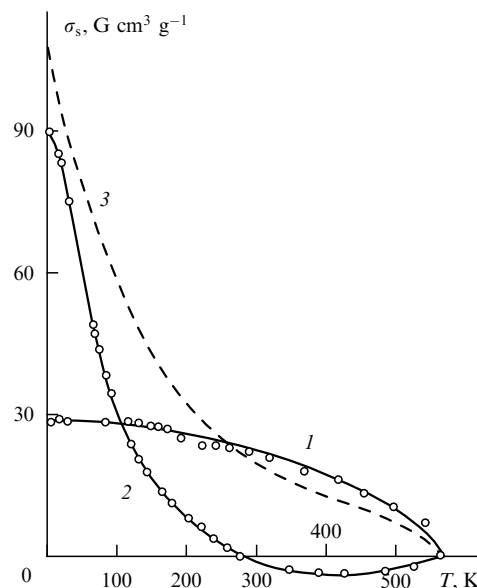
Out task here is, based on the experimental Gd₃Fe₅O₁₂ and Y₃Fe₅O₁₂ $I_s(T)$ curves, to find the temperature dependence of I_s for the gadolinium (*c*) sublattice. This can be achieved by noting the following. The exchange interaction between the *c* and *ad* sublattices is negative, hence the pertinent magnetizations are related by

$$I_{s,c} - I_{s,ad} = I_s^{\text{result}}.$$

From this, substituting for $I_{s,ad}$ the value of I_s for Y₃Fe₅O₁₂, and for I_s^{result} the I_s for the experimental Gd₃Fe₅O₁₂ curve, the I_s of the gadolinium sublattice is found to be

$$I_{s,\text{Gd}} = I_{s,\text{Y}_3\text{Fe}_5\text{O}_{12}} + I_{s,\text{Gd}_3\text{Fe}_5\text{O}_{12}}.$$

The curves 1 and 2 in Fig. 1 represent the experimental temperature dependences of the specific spontaneous magnetization of Y₃Fe₅O₁₂ and Gd₃Fe₅O₁₂. (Since the magnetization σ_s of Gd₃Fe₅O₁₂ changes sign on passing through Θ_c , the corresponding σ_s ’s are plotted in a negative quadrant.) To obtain $\sigma_s^{\text{Gd}}(T)$ curve of the gadolinium sublattice, it is necessary to add the ordinates of the curves 1 and 2 in Fig. 1. The result of this graph addition is the dashed curve 3, which shows exactly the $\sigma_s^{\text{Gd}}(T)$ dependence. It is seen that, starting from the lowest temperatures, the spontaneous magnetization of the gadolinium sublattice exhibits an exponential

**Figure 1.** The temperature dependence of the specific spontaneous magnetization: 1 — yttrium–iron garnet Y₃Fe₅O₁₂; 2 — Gd₃Fe₅O₁₂; 3 — ‘weak’ (gadolinium) sublattice.

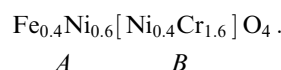
decay with temperature. This behaviour differs sharply from that of the *ad* (‘strong’) sublattice. Rather, it resembles — but still differs from — the curve observed in ordinary Curie–Weiss paramagnetic materials (see below).

From Fig. 1 it can be seen that the point Θ_c appears at the temperature of intersection of the curves 1 and 3, implying that one sublattice of the ferrimagnet is ‘weak’ and that its low-temperature magnetization exceeds that of the ‘strong’ sublattice.

Clearly, in the intermetallides HoFe₃, ErFe₂, etc., one can separate out a ‘weak’ sublattice in a similar way, i.e. by graphically adding the experimental $I_s(T)$ [or $\sigma_s(T)$] curves for these substances and those for YFe₃ and YFe₂.

The situation in ‘diluted’ spinel ferrites (see Table 1) is more difficult in that, for these, the graph addition procedure outlined above cannot be applied to the sublattice $I_s(T)$ curves. The point is that in spinel ferrites the Fe³⁺ cations may be present in both the *B* and *A* sublattices and thus in most cases the iron (‘strong’) sublattice cannot be separated in a pure form as was the case for Gd₃Fe₅O₁₂. However, indirect evidence for the existence of a ‘weak’ sublattice in these ferrites comes from the shape of the magnetization versus temperature curves below Θ_c . This is seen from Fig. 2 which presents the magnetization curve $\sigma(T)$ measured in the saturation field H_s for the spinel ferrite NiFe_{0.4}Cr_{1.6}O₄ [16] with a Θ_c point. It is seen that at $T < \Theta_c$, the $\sigma(T)$ curve exhibits a fast decay similar to that observed in Gd₃Fe₅O₁₂ in the corresponding temperature range.

In diluted spinel ferrites the ‘weak’ sublattice is generally the octahedral (*B*) sublattice, and the ‘strong’ sublattice, the tetrahedral (*A*) sublattice. The cation distribution in, for example, the Θ_c -point-possessing ferrite NiFe_{0.4}Cr_{1.6}O₄ takes the form [19]



Given the electronic configurations of the *B*- and *A*-site cations in this ferrite [Fe³⁺(3*d*⁵), Ni²⁺(3*d*⁸), and Cr³⁺(3*d*³)],

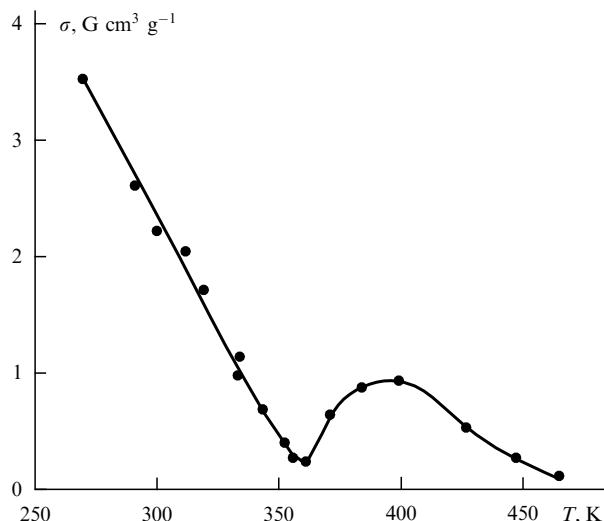


Figure 2. The temperature dependence of the specific magnetization σ (at saturation) for the spinel ferrite $\text{NiFe}_{0.4}\text{Cr}_{1.6}\text{O}_4$.

one can estimate the sublattice magnetizations (the cation Fe^{3+} has no orbital momentum, whereas in Ni^{2+} and Cr^{3+} the latter is crystal-field-frozen). The spin magnetic moment at 0 K is $5.6\mu_B$ and $3.2\mu_B$ for the B and A sublattices, respectively. At the same time the exchange interaction of the B -sublattice Ni^{2+} and Cr^{3+} cations is much smaller than that of the A -sublattice Fe^{3+} and Ni^{2+} cations (large exchange interaction is always due to there being many Fe^{3+} cations). Thus, the situation resembles that in $\text{Gd}_3\text{Fe}_5\text{O}_{12}$, and hence the presence of a 'weak' B sublattice gives rise to the Θ_c point in this spinel ferrite.

The existence of the Θ_c point in spinel ferrites is accounted for [1, 20] by assuming that both sublattices have very nearly Weiss-type $I_s(T)$ curves (i.e. both are 'strong'). In this case, however, the $I_s(T)$ addition procedure described above implies that Θ_c must be close to the Curie point T_C , so that this assumption does not allow one to explain the appearance of Θ_c points in rare-earth–iron garnets, in which these points are far away from T_C . Nor does it account for the strong low-temperature paraprocess (see below) characteristic of ferrimagnets with a Θ_c point.

Now what is the reason for the existence of a 'weak' magnetic sublattice in the ferromagnets we are considering? In order to answer this question, it is necessary to analyze exchange interactions in these materials. This has been done for gadolinium–iron garnet, both stoichiometric and containing substitutional nonmagnetic cations. Although the inter- and intrasublattice exchange interactions for the substitutional cations have been determined by various methods, the molecular field method has been most frequently used for the purpose.

Table 2 lists the molecular-field values of the exchange integrals for the $\text{Y}_3\text{Fe}_5\text{O}_{12}$ and $\text{Gd}_3\text{Fe}_5\text{O}_{12}$ ferrites [21–23].

Table 2. Values of the exchange interaction integrals J_{ad} , J_{dd} , and J_{aa} (in kelvins) for the iron garnets $\text{Gd}_3\text{Fe}_5\text{O}_{12}$ and $\text{Y}_3\text{Fe}_5\text{O}_{12}$

Ferrite	J_{ad}	J_{dd}	J_{aa}	Ref.
$\text{Gd}_3\text{Fe}_5\text{O}_{12}$	–35.8	–15.0	–8.2	[21]
$\text{Y}_3\text{Fe}_5\text{O}_{12}$	–34.8	–14.8	–8.3	[22]
	–36.3	–14.8	–8.8	[23]

It is seen from the table that the values of J_{ad} , J_{dd} , and J_{aa} in these ferrites do not differ substantially, confirming what have previously been said about these interactions.

In addition, Table 3 lists the values of the integrals J_{cc} , J_{dc} , and J_{ac} for $\text{Gd}_3\text{Fe}_5\text{O}_{12}$ as found by the molecular field and other techniques.

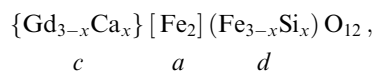
Table 3. $\text{Gd}_3\text{Fe}_5\text{O}_{12}$ exchange interaction integrals J_{dc} , J_{ac} , and J_{cc} (in kelvins) as obtained by different methods

Method	J_{dc}	J_{ac}	J_{cc}	Ref.
Molecular field	–3.7	–0.44	0	[23]
Molecular field	–4.8	–0.32	–0.22	[24]
NMR	–4.1	0	–0.043	[25]
Mössbauer effect	—	—	–0.13	[26]

It follows from this table that J_{cc} and J_{ac} are extremely small and play a negligible role in the magnetic ordering of the Gd^{3+} cations in the c sublattice.

A different situation occurs for the interaction of the d and c sublattices. Although the value of J_{dc} is also small compared to J_{ad} (this interaction produces the $T_C = 556$ K Curie point in $\text{Gd}_3\text{Fe}_5\text{O}_{12}$, see Table 1), nonetheless J_{dc} is about 12% of J_{ad} . Molecular field calculations [27] of the effective exchange field H_{ex} induced by the iron sublattices (mainly by the d -sublattice Fe^{3+} cations) yield $\sim 3 \times 10^5$ Oe, close to the value derived from the magnetocaloric effect in $\text{Gd}_3\text{Fe}_5\text{O}_{12}$ ($H_{ex} = 2.58 \times 10^5$ Oe) [28]. Since this is an order of magnitude less than the exchange field due to J_{ad} interactions ($H_{ex} \sim 10^6$ Oe), one is justified in using the term 'weak' for the Gd sublattice.

In order to develop a better understanding of the 'weak' sublattice problem, let us consider results on the gadolinium–iron garnet with substitutional nonmagnetic cations. In [21], the magnetic properties of the system



where $x = 0, 0.3, 0.6, 0.9$, and 1.2 , were examined. Since the a sublattice interacts weakly with the c sublattice, the focus of attention was on how the d sublattice affects H_{ex} . The value of H_{ex} was calculated using the molecular field expression for the c sublattice magnetization [27]

$$I_c = I_{0c} B_s \frac{\mu_B \cdot 2SH_{ex}}{kT},$$

where I_c is the magnetization of the c sublattice induced by the exchange field of the d sublattice, B_s is the Brillouin function, and S , the spin of the Gd^{3+} cation.

In Fig. 3 are shown the $H_{ex}(T)$ dependences calculated from this formula [21] for various compositions of substituted gadolinium–iron garnets. The value of H_{ex} decreases dramatically with the concentration of nonmagnetic cations, presumably due to the breaking of the Gd^{3+} – Fe^{3+} exchange bonds. The 'weak' temperature dependence of H_{ex} is resulted from the Weiss nature of the I_s for the d sublattice away from T_C .

The above formula also yields the temperature dependences $M_{s,c}$ of a 'weak' (c) sublattice (Fig. 4). It is seen that as x increases, the slope of the exponentially falling curve $M_{s,c}(T)$ decreases, meaning that the 'weak' c sublattice gradually 'transforms' to a paramagnetic state due to a decrease in H_{ex} . Thus, the paramagnetic sublattice differs from the 'weak' sublattice in that the latter has its cations

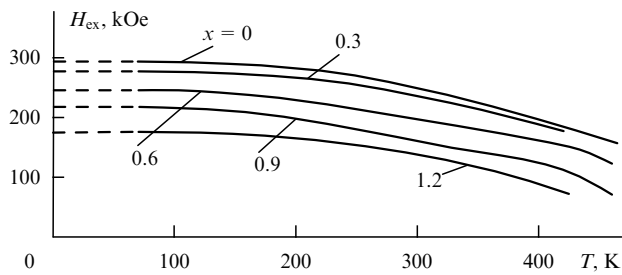


Figure 3. The temperature dependence of H_{ex} for the iron garnet system $\text{Gd}_{3-x}\text{Ca}_x\text{Fe}_{5-x}\text{Si}_x\text{O}_{12}$.

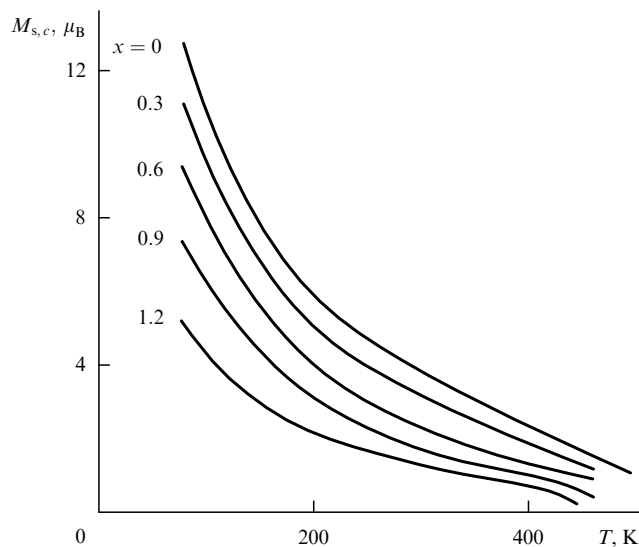


Figure 4. Temperature dependences of the gadolinium sublattice spontaneous magnetization [the ordinate axis presents magnetic moments $M_{s,c}$ (in units of μ_B) per $\text{Gd}_3\text{Fe}_5\text{O}_{12}$ ferrite formula unit].

subject to a by far stronger exchange field H_{ex} , i.e. possesses ‘exchange-enhanced’ paramagnetism in a sense.

3. Low-temperature paraprocess and ‘low-temperature point’ T_B in a ‘weak’ sublattice

The paraprocess differs from paramagnetic magnetization in that, owing to the presence of strong spin exchange correlation in the substance, the application of an external magnetic field H causes a larger magnetization increase compared to a paramagnet. In an ordinary ferromagnet, the paraprocess is ‘weak’ at low temperatures — because the number of thermally disoriented spins is small — and very strong near the Curie point, where this number is large. A further reason why the magnetization enhancement in this region is large is that the orienting effect of H may influence not only individual spins but also groups of spins ‘correlated’ by the exchange interaction. The above reasoning suggests the ‘exchange-enhanced paramagnetism’ as a definitive term for the paraprocess.

In a ferrimagnet with a Weiss-type temperature dependence $I_s(T)$ (Néel’s Q curve), the paraprocess proceeds exactly as in ordinary ferromagnets provided the competition between sublattice exchange interactions does not give rise to a noncollinear magnetic structure. If it does, the ferrimagnet exhibits a strong paraprocess as a result of the

‘destruction’ of this structure by the field H . However, in ferrimagnets with a ‘weak’ sublattice there is no competition between sublattice exchange interactions and hence no conditions for the development of a noncollinear magnetic structure. There is a ‘one-way’ H_{ex} field of the ‘strong’ sublattice exerting on the magnetic cations of its ‘weak’ counterpart.

Notice that early in the investigation of the low-temperature paraprocess [6] the ‘weak’ sublattice of $\text{Gd}_3\text{Fe}_5\text{O}_{12}$ revealed a maximum in the paraprocess susceptibility χ_p at $T_B \sim 100$ K. The appearance of a maximum on the $\chi_p(T)$ curve was explained [2, 3, 27] with the assumption that the thermal motion at this temperature causes a partial but sharp change in the magnetic order in a ‘weak’ sublattice (the authors called the ‘weak’ sublattice T_B a ‘low-temperature point’). This change leads to a slight kink in the $I_s(T)$ curve of the iron garnet in the T_B vicinity.

As mentioned above, the exchange integral J_{cd} is about 12% less than J_{ad} and hence for $\text{Gd}_3\text{Fe}_5\text{O}_{12}$ with the Curie point $T_C = 556$ K, T_B must be approximately 67 K. While a somewhat higher experimental value was first reported [6], later on [7] paraprocess magnetostriction ($\partial\lambda_p/\partial H$) and susceptibility (χ_p) measurements on $\text{Gd}_3\text{Fe}_5\text{O}_{12}$ yielded $T_B = 70$ K in accordance with the above estimate. In [7], T_B values for other iron garnets of heavy rare-earth metals were also measured (see Table 1). As an example, Fig. 5 depicts the temperature dependences of $\partial\lambda_p/\partial H$ and χ_p for $\text{Ho}_3\text{Fe}_5\text{O}_{12}$; for this ferrite the authors of [7] estimated $T_B = 32$ K.

The problem of the appearance of T_B points in a ‘weak’ sublattice of rare-earth–iron garnets has been analyzed in

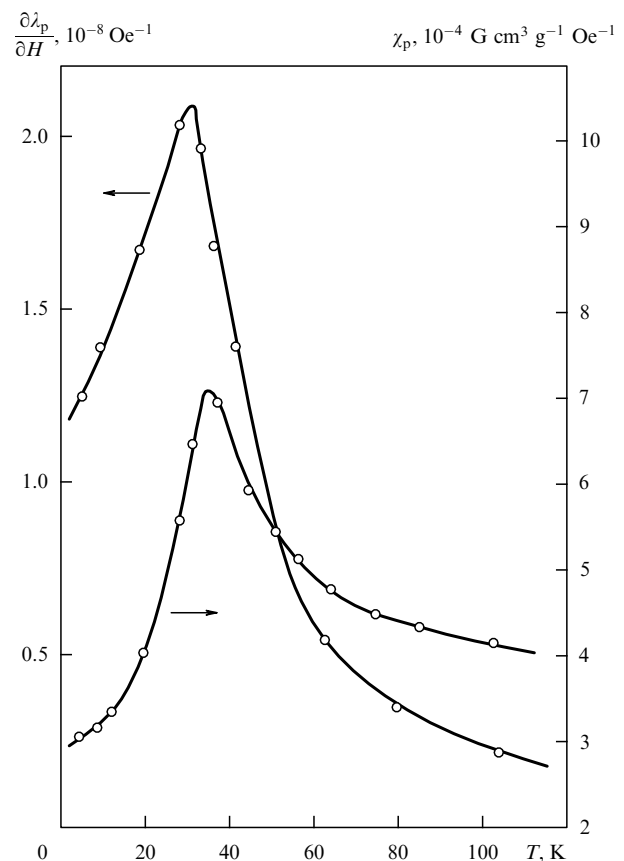


Figure 5. Temperature dependences of the paraprocess susceptibility and paraprocess magnetostriction for $\text{Ho}_3\text{Fe}_5\text{O}_{12}$ at $H = 23$ kOe.

terms of molecular field theory [27]. The calculations left out an account of the exchange integral J_{cc} and the back action of the rare-earth cations on the d sublattice, i.e., in a sense, only one-way action of Fe^{3+} cations on R^{3+} was considered. This implies that the exchange energy, and hence the magnetostriiction of the paraprocess, is taken to be proportional to the first power of magnetization.

The $\lambda_p(\sigma)$ versus specific magnetization σ curve substantiates this conclusion (Fig. 6) [7]. Notice that the magnetocaloric effect in $\text{Gd}_3\text{Fe}_5\text{O}_{12}$ also shows a linear dependence on σ [30]. Thus, the 'parity' of these effects is violated in ferrimagnets with a 'weak' sublattice.

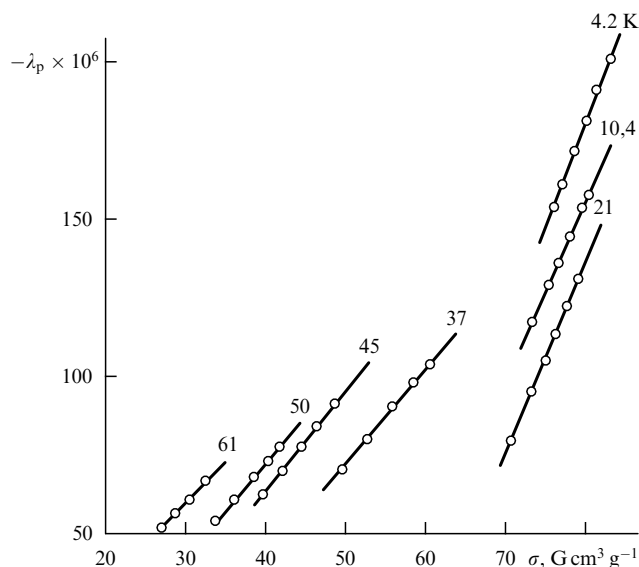


Figure 6. The dependence of the paraprocess magnetostriction λ_p on the magnetization for $\text{Ho}_3\text{Fe}_5\text{O}_{12}$.

The expression for T_B obtained in [27] is as follows

$$T_B \propto \frac{\mu_B g_s S H_{ex}}{k},$$

where S is the spin of the rare-earth cation. Since H_{ex} 's are about the same in all rare-earth–iron garnets (the same ad sublattices), this is the only factor to determine T_B . Figure 7 presents the S -dependences of T_B , both calculated from the above formula (within a numerical constant) and determined experimentally [7] from the positions of $\partial\lambda_p/\partial H$ and χ_p maxima. It is seen that the theoretical predictions agree with the experimental results.

In Ref. [16], a low-temperature T_B point was found in $\text{Li}_{0.5}\text{Fe}_{1.25}\text{Cr}_{1.25}\text{O}_4$ ferrite with a Θ_c point. From Fig. 8, $T_B \sim 102$ K.

Experiments [9] on intermetallic compound HoFe_3 place the low-temperature paraprocess susceptibility maximum at $T_B \sim 170$ K (Fig. 9), which is higher than in rare-earth–iron garnets or in the above-mentioned spinel ferrite. The reason is that in rare-earth–iron intermetallides the R–Fe exchange interaction is stronger than in iron garnets and spinel ferrites, and the iron sublattice exchange field 'induces' a higher T_B .

The existence of the T_B point in a 'weak' sublattice of a ferrimagnet was predicted by the present author in 1961 [2, 3] and has subsequently been discovered in a number of ferrimagnets (see Table 1). The lack of data on T_B for most rare-earth–iron(cobalt) intermetallides and substituted ferrites

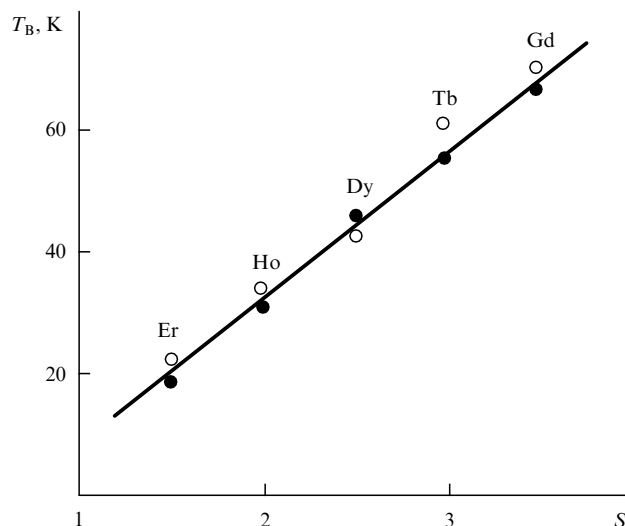


Figure 7. The dependence of the iron garnet T_B on the rare-earth cation spin: \circ — theory; \bullet — experiment.

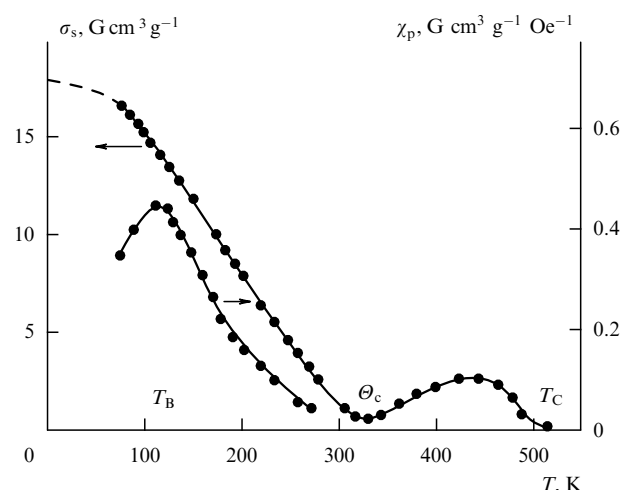


Figure 8. The temperature dependence of the paraprocess susceptibility χ_p for the $\text{Li}_{0.5}\text{Fe}_{1.25}\text{Cr}_{1.25}\text{O}_4$ ferrite near the Θ_c point.

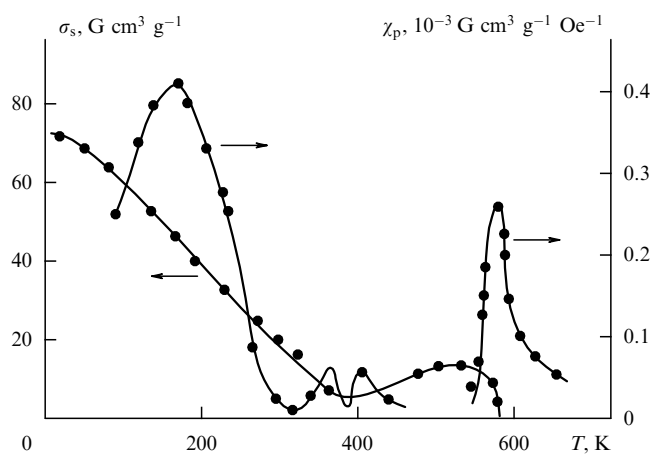


Figure 9. Temperature dependences of σ_s and χ_p for the HoFe_3 intermetallide near T_B and T_C .

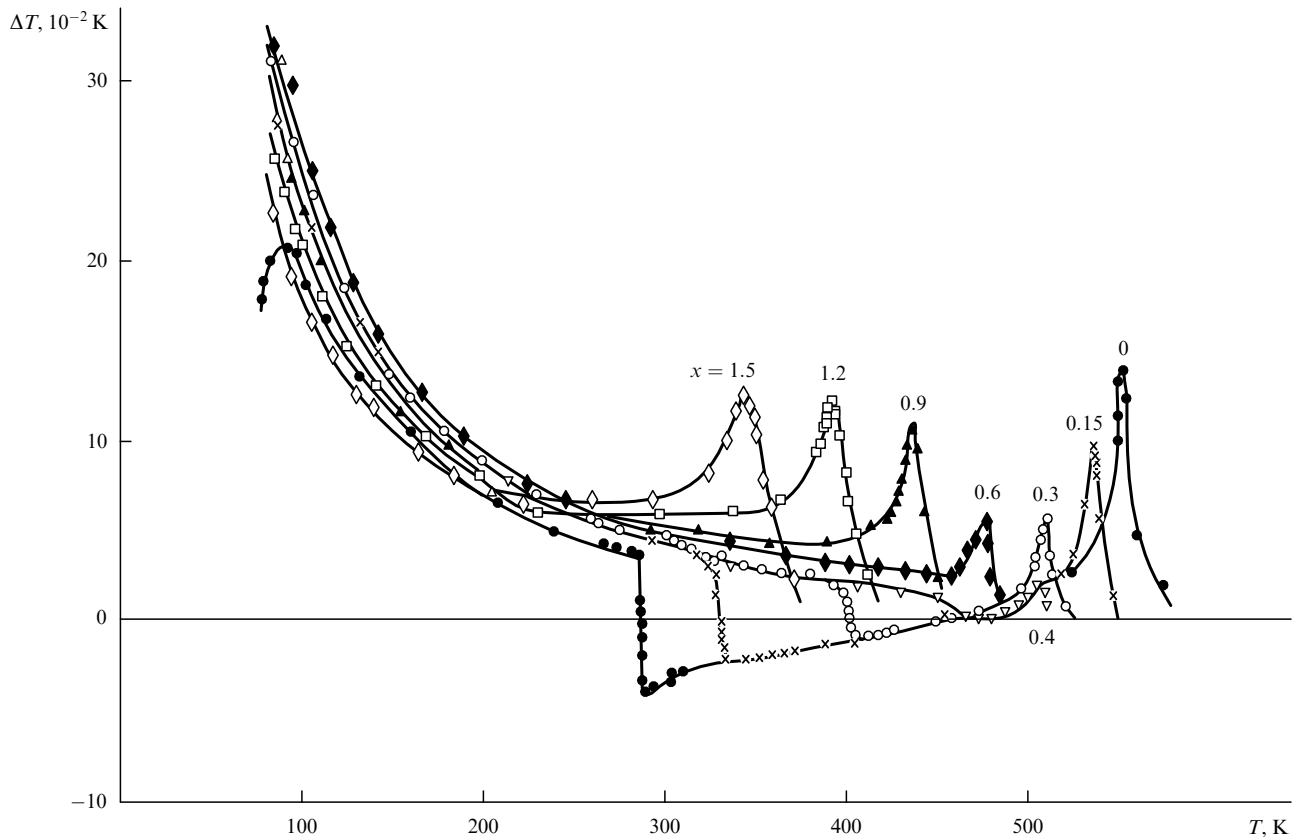


Figure 10. Temperature dependences of the magnetocaloric effect for substitutional iron garnets $\text{Gd}_3\text{Ca}_x\text{Fe}_{5-x}\text{O}_{12}$ ($x = 0 - 1.5$) at $H = 16$ kOe.

is presumably due to the fact that no relevant measurements are available.

It was argued [2, 3] that T_B is not to be identified with the ordinary Curie point T_C . The existence of T_B is not due to the ‘intrinsic’ exchange interaction in a ‘weak’ sublattice — or in the case of $\text{R}_3\text{Fe}_5\text{O}_{12}$ ferrites, not due to the J_{cc} exchange integral — but rather is determined by the intersublattice exchange interaction (J_{dc} contribution). The transition at T_B is, in a sense, ‘induced’ by the exchange field H_{ex} of the neighbouring ‘strong’ sublattice.

The difference between T_B and T_C is that in transiting at T_B the spontaneous magnetization I_s in a ‘weak’ sublattice does not disappear, as is the case at T_C , but remains finite and only undergoes a sharp change in magnitude. For the T_B region, the distinguishing feature is, as we have seen above, that the paraprocess magnetostriction $\partial\lambda_p/\partial H$ and the magnetocaloric effect ΔT , for example, are linear in I_s , whereas near T_C they are proportional to I_s^2 . The question to be answered in subsequent investigations is whether the magnetic phase transition at T_B is of the second order, and what exactly is the role of magnetic-order fluctuations (i.e. critical state) in the transition at T_B . This problem is discussed in a recent monograph [29], in which the T_B point is called the ‘low-temperature Belov point’.

Since at $T > T_B$ the ‘weak’ sublattice maintains much of its magnetic order, it follows that the low-temperature paraprocess must manifest itself at these temperatures as well, including the vicinity of Θ_c . This paraprocess is the main culprit for the various anomalous effects seen in the magnetic compensation point vicinity.

In the Θ_c region, the magnetocaloric effect (ΔT -effect) changes sign. Figure 10 presents ΔT -effect data [30, 31] on the

system of substitutional gadolinium–iron garnets $\text{Gd}_3\text{Fe}_5\text{O}_{12}$. A change in the sign of ΔT at $T = \Theta_c$ is seen. At $T < \Theta_c$, where the magnetization \mathbf{I} of the gadolinium sublattice is along the external field \mathbf{H} , an ordinary ferromagnet-type paraprocess occurs, which decreases the magnetic component of the entropy (magnetic order increases upon application of H), and this decrease, in turn, results in a normal (positive) sign of the ΔT -effect. For $T > \Theta_c$, the gadolinium sublattice \mathbf{I} is opposite to \mathbf{H} and an antiferromagnet-type paraprocess takes place (field \mathbf{H} ‘turns’ \mathbf{I}_{Gd} by 180°), which increases the magnetic entropy component and thus gives rise to a negative ΔT -effect, that is, the sign of the ΔT -effect reverses in passing Θ_c . Similar ΔT sign changes on passing Θ_c were observed in ErFe_2 and HoFe_3 intermetallide compounds [32].

The behaviour of isotropic (paraprocess-induced) magnetoresistance near Θ_c was studied in lithium chromite ferrite [33–35]. Figure 11 depicts the temperature dependences of the longitudinal effect $(\Delta\rho/\rho)_\parallel$ near Θ_c [$(\Delta\rho/\rho)_\perp$ curves are identical]. It is seen that on passing Θ_c the sign of $(\Delta\rho/\rho)_\parallel$ changes from negative to positive. This is due to the paraprocess of an antiferromagnet type occurring in a ‘weak’ sublattice at $T > \Theta_c$ [36]. In a ferromagnet-type process, the scattering of current carriers off the magnetic order decreases (giving rise to a negative $\Delta\rho/\rho$), whereas in the antiferromagnetic case it increases ($\Delta\rho/\rho$ is positive).

There is a report [37] on a change in the sign of the paraprocess magnetostriction $\partial\lambda_p/\partial H$ at the Θ_c point of dysprosium–iron garnet $\text{Dy}_3\text{Fe}_5\text{O}_{12}$.

Both beyond and below Θ_c , the paraprocess and its concomitant phenomena we have described above are due to a ‘weak’ sublattice. The ‘strong’ sublattice plays here only a passive role.

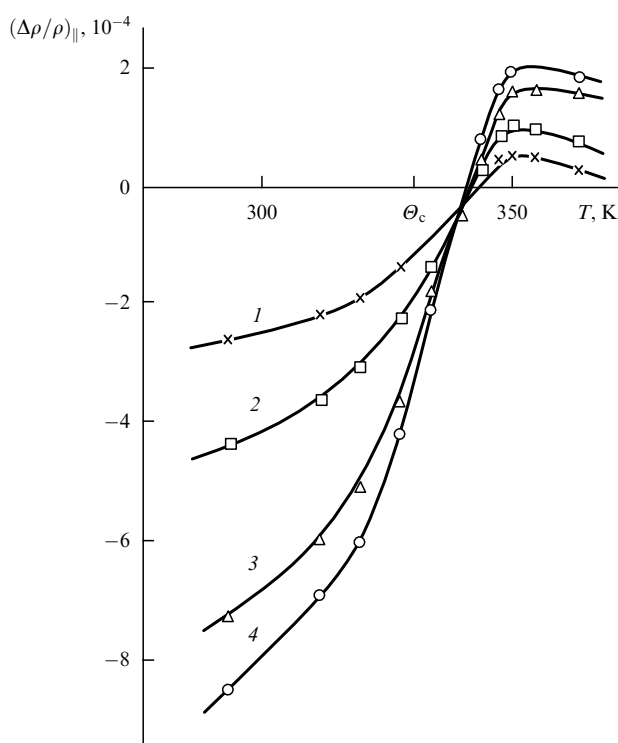


Figure 11. The isotropic magnetoresistance of $\text{Li}_2\text{O}(\text{Fe}_2\text{O}_3)_{2.5}(\text{Cr}_2\text{O}_3)_{2.5}$ ferrite near Θ_c at $H = 2.26$ (1); 4.5 (2); 9.03 (3); 11.07 kOe (4).

A change in the sign of the isotropic magnetoresistance was observed [39, 40] in the metallic ferrimagnet Mn_5Ge_2 on passing the $\Theta_c \sim 400$ K point and interpreted by means of a phenomenological theory [41]. In this theory, the galvanomagnetic properties of ferri- and antiferromagnets depend on two vectors: the ferromagnetism vector $\mathbf{M} = \mathbf{M}_1 + \mathbf{M}_2$ (where \mathbf{M}_1 and \mathbf{M}_2 are the sublattice magnetizations) and the antiferromagnetism vector $\mathbf{L} = \mathbf{M}_1 - \mathbf{M}_2$, i.e. these substances display two galvanomagnetic effects of opposite sign, one corresponding to the vector \mathbf{M} , and another, to \mathbf{L} . While the vector \mathbf{M} vanishes at the Θ_c point, \mathbf{L} does not, and it is the galvanomagnetic effect due to this latter which was observed in Refs [39, 40] (the magnetoresistance and Hall electromotive force changed sign on passing through Θ_c).

The interpretation of the magnetoresistance sign change and other effects in terms of the antiferromagnetic paraprocess was given in 1961 [2, 3], and the above phenomenological picture was proposed in 1962, that is, at practically the same time. In our view, the former approach is more transparent physically, however.

There have been a number of detailed studies, both theoretical and experimental, of the noncollinear magnetic structure induced by an external field H near the Θ_c point [42–44]. The structure arises from the fact that on the one hand there is a negative exchange interaction between sublattices (c and da in the $\text{Gd}_3\text{Fe}_5\text{O}_{12}$ case), which tends to make their moments aligned antiparallel, and on the other, the interaction between the sublattices and the field \mathbf{H} , which aligns their moments along the field (and hence mutually parallel). The reason for the interest in this phenomenon is that it provides a good example to study the properties of a new class of magnetoorientation magnetic phase transitions. The relevant results are discussed in detail in a monograph [43] and need not be repeated here. We wish, however, to

emphasise the 'active' role of a 'weak' sublattice in the formation of the induced magnetic structure: upon application of \mathbf{H} , its magnetic moment grows (due to the paraprocess) and at $\mathbf{H} = \mathbf{H}_{cr}$ begins to compete (provided negative sublattice exchange interaction) with the magnetic moment of a 'strong' sublattice (ad in iron garnets); the latter moment remains virtually unchanged in the course of the noncollinear structure formation process and thus plays a passive role.

An intensive low-temperature paraprocess, together with its concomitant effects, has also been observed at temperatures other than Θ_c , both beyond and above it. In the Gd, Tb, Dy, and Ho iron garnets, it has been shown [38] that between 280 and 100 K, in addition to anisotropic magnetostriction, strong isotropic $\partial\lambda_p/\partial H$ magnetostriction arises as a result of a 'weak' sublattice paraprocess. Large ΔT -effects at $T < \Theta_c$ in $\text{Gd}_3\text{Fe}_5\text{O}_{12}$ and in substitutional iron garnets $\text{Gd}_3\text{Ca}_x\text{Fe}_{5-x}\text{O}_{12}$ have been reported [30, 31] for $0 \leq x \leq 1.5$ (see Fig. 10).

4. 'Weak' sublattice in ferrimagnets with an anomalous temperature behaviour of the spontaneous magnetization (Néel's M and P curves)

Néel's theory [1] implies that ferrimagnets must exist in which, unlike ferromagnets, spontaneous magnetization does not increase but rather decreases as the temperature reduces and tends to 0 K (M and P curves in the Néel's notation). As in ferrimagnets with a magnetic compensation point, it turns out [2, 3] that such dependences are most favoured in 'weak' sublattice ferrimagnets.

Figure 12a illustrates schematically the $I_s(T)$ dependence of a 'weak' sublattice of one of the ferrimagnets under study; notice that I_s decreases exponentially with temperature (curve 2) and that the magnetization of this lattice is at all temperatures less than that of the 'strong' one (curve 1). Curve 3 presents the experimentally observed temperature behaviour of I_s (Néel's M curve). (In the special case where the zero-temperature magnetizations of the 'weak' and 'strong' sublattices are equal in magnitude, the Néel's L curve emerges.)

M -type $I_s(T)$ dependences have been detected in rare-earth–cobalt and rare-earth–iron intermetallides. Figure 13 reproduces the data from Ref. [45] on temperature dependences of magnetic moments M_s per formula unit (in Bohr magnetons) in R_2Co_{17} compounds. It is seen that if in compounds with light rare-earth metals the dependences $M_s(T)$ are of the ferromagnet Weiss form, in intermetallides with heavy rare-earth metals they have the form of an M -type curve.

Figure 14 presents the data, from the same study, on the dependences of relative magnetization $M_s(T)/M_s(0)$ ($M_s(0)$ is the spontaneous magnetization at 0 K) for rare-earth sublattices of intermetallides R_2Co_{17} (R being a heavy rare-earth metal). As in the case of $\text{Gd}_3\text{Fe}_5\text{O}_{12}$, these dependences exhibit an exponential decrease implying that rare-earth sublattices are 'weak'. It is found that for the Gd intermetallide the $M_s(T)/M_s(0)$ dependence is given by a simple Brillouin function, whereas for intermetallides of Tb, Dy, etc., the anisotropic molecular field relations are needed [46], since in these compounds the exchange interaction is comparable with the magnetocrystalline anisotropy energy (see also [11]). However, as seen from Fig. 14, the Tb and Dy sublattices still remain 'weak'.

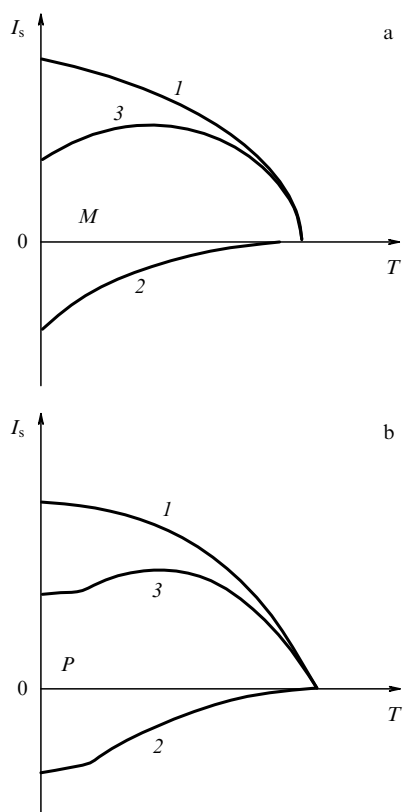


Figure 12. $I_s(T)$ dependences of the Néel's M and P type.

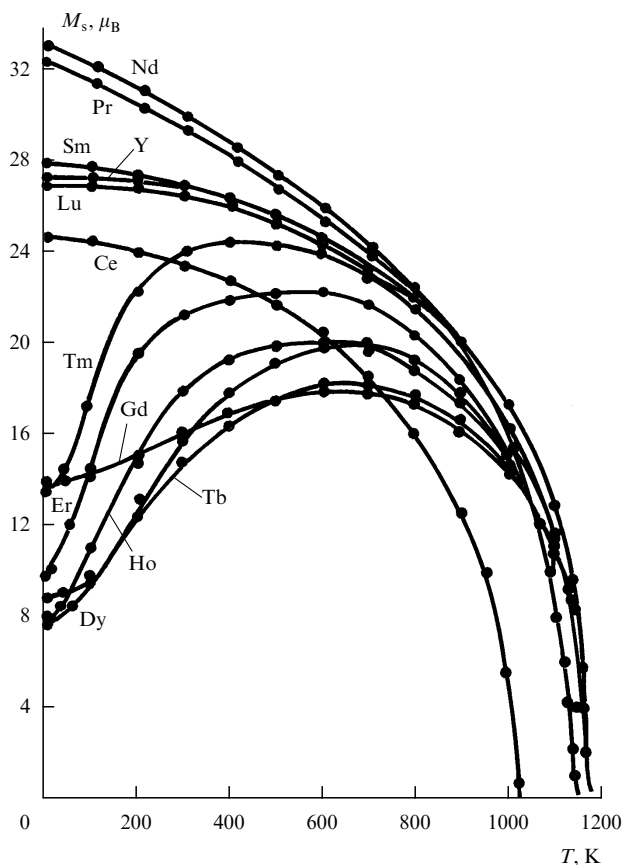


Figure 13. Behaviour of magnetic moments M_s per formula unit (in μ_B) for R_2Co_{17} intermetallics.

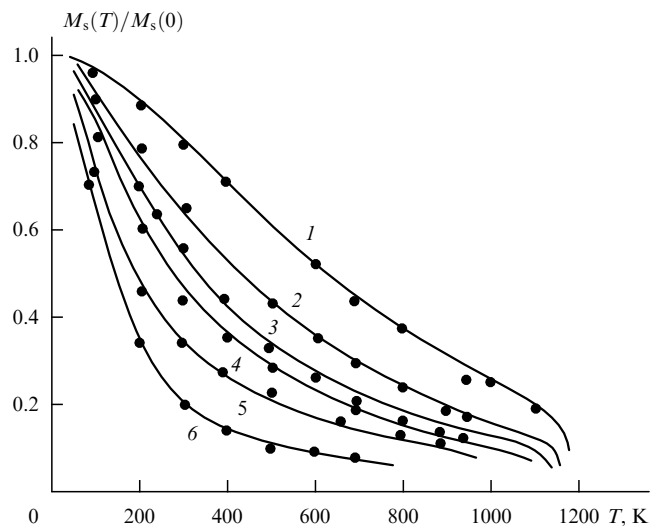


Figure 14. Behaviour of the relative magnetization $M_s(T)/M_s(0)$ in the rare-earth sublattice of R_2Co_{17} compounds: 1 — R = Gd, 2 — Tb, 3 — Dy, 4 — Ho, 5 — Er, 6 — Tm.

M -type $I_s(T)$ dependences have also been observed in the iron garnets of heavy rare-earth metals. An example is the yttrium–iron garnet $Y_3Fe_5O_{12}$ with nonmagnetic cations Y^{3+} partly substituted by Tb^{3+} cations [47]. Figure 15 presents temperature dependences of specific spontaneous magnetization in the $Y_{3-x}Tb_xFe_5O_{12}$ system. The $x = 0.1$ and 0.3 samples show M -type $\sigma_s(T)$ dependences. At larger values of x , as seen in Fig. 15, N -type dependences arise. M -type curves have also been found in Li–Al spinel ferrites (Fig. 16) [48].

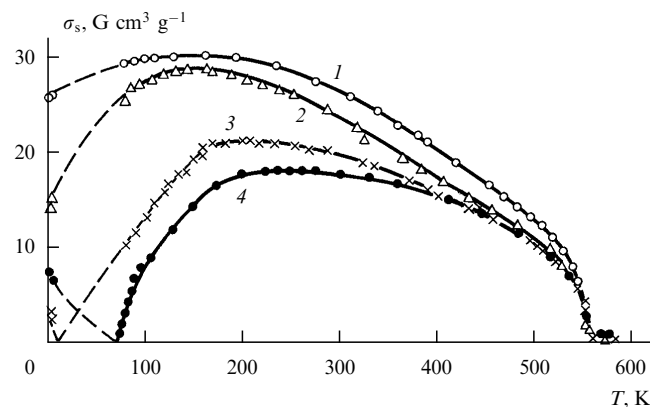


Figure 15. Dependence $\sigma_s(T)$ for the iron garnet $Y_{3-x}Tb_xFe_5O_{12}$ system: 1 — $x = 0.1$; 2 — 0.3; 3 — 0.8; 4 — 1.

Ferrimagnets, however, may show $I_s(T)$ dependences somewhat different from the M -type curves, namely Néel's P -type curves (Fig. 12b). Such a dependence arises when close to 0 K the 'weak' sublattice is 'well' ordered, i.e. curve 2 in Fig. 12b has a nearly 'horizontal' portion. 'Subtracting' this curve from curve 1 then yields a P -type curve. Such $I_s(T)$ dependences arise in ferrimagnets whose 'weak' sublattice is affected relatively heavier by the 'strong' sublattice. Dependences like this are indeed surveyed experimentally. Figure 17, after [49], shows the $\sigma_s(T)$ dependence for Tm_6Fe_{23} intermetallic. It is seen that the $\sigma_s(T)$ curve has a nearly horizontal portion near 0 K.

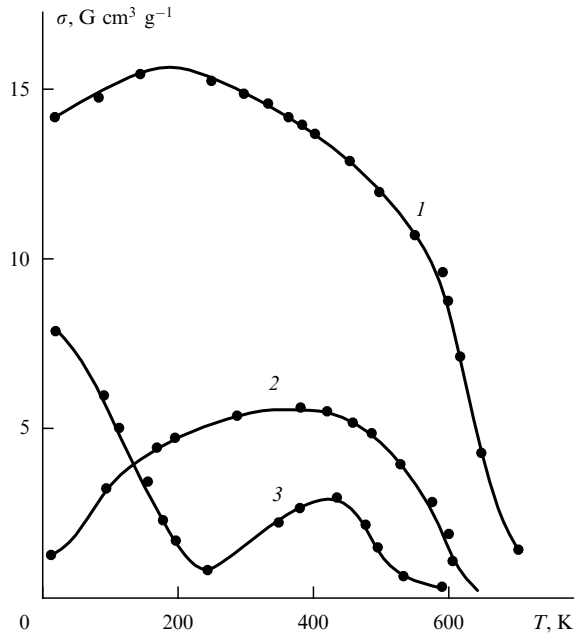


Figure 16. Temperature dependences of magnetization (at saturation): 1 — $\sigma_s(T)$ for the $\text{Li}_{0.5}\text{Fe}_{1.9}\text{Al}_{0.6}\text{O}_4$ ferrite; 2 — $\sigma(T)$ in a field of 10.6 kOe for the $\text{Li}_{0.5}\text{Fe}_{1.7}\text{Al}_{0.8}\text{O}_4$ ferrite; 3 — $\sigma(T)$ for $\text{Li}_{0.5}\text{Fe}_{1.5}\text{AlO}_4$ at 10.6 kOe.

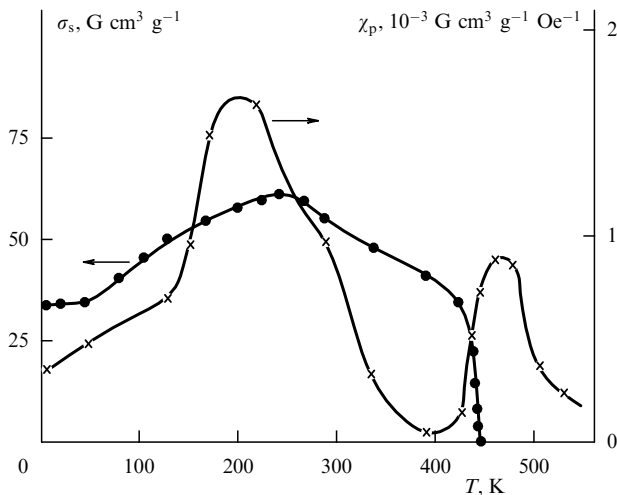


Figure 17. Temperature dependences of specific spontaneous magnetization σ_s and the paraproduct susceptibility χ_p for the $\text{Tm}_6\text{Fe}_{23}$ compound.

Clearly, as is the case of ferrimagnets with magnetic compensation point, in ferromagnets with *M*- and *P*-type curves the 'weak' sublattice must give rise to low-temperature T_B points and to a low-temperature paraproduct. These must be of an antiferromagnet type because in the ferromagnets under study the applied field H acts to orient the I_s of a 'strong' sublattice, and hence that of a 'weak' sublattice will be oriented opposite to H .

From Fig. 17, which along with σ_s presents data on the paraproduct susceptibility χ_p for $\text{Tm}_6\text{Fe}_{23}$ [49], it is seen that at ~ 200 K χ_p displays a maximum by far exceeding that at the Curie point. The authors of Ref. [49] derive it from the existence of a T_B point in that particular material.

The existence of the antiferromagnet paraproduct in ferrimagnets with the Néel's *M*-type $I_s(T)$ dependence is experimentally confirmed by the anomalous (negative) sign

of the magnetocaloric effect [50, 51]. Another piece of evidence comes from the fact that in the Li-Ti spinel ferrite with an *M*-type $I_s(T)$ dependence, $\partial\lambda_p/\partial H$, i.e. the paraproduct magnetostriction, has an anomalous (negative) sign [53], whereas in other ferromagnet-paraproduct ferrites $\partial\lambda_p/\partial H > 0$.

Figure 18 presents experimental results on the specific spontaneous magnetization and isotropic (i.e. paraproduct-related) magnetoresistance $\Delta\rho/\rho$ for the $\text{Li}_{0.5}\text{Fe}_{1.7}\text{Al}_{0.8}\text{O}_4$ ferrite [52]. This ferrite has an *M*-type $\sigma_s(T)$ curve. In addition to the isotropic magnetoresistance maximum at T_C , there is a larger $\Delta\rho/\rho$ maximum at ~ 480 K, where a kink in the $\ln R(1/T)$ curve also occurs (see insert to Fig. 18). The corresponding kink at T_C is too small to be detected. An attempt has been made [52] to interpret the 480 K-maximum as being due to the paraproduct which results from the destruction of a noncollinear magnetic structure by H . There is however no reason to believe that such a structure exists in this particular ferrite, since the *M*-type $\sigma_s(T)$ dependence in it is more reasonably attributable to the appearance of a $\Delta\rho/\rho$ maximum at the T_B point. But the maximum of the isotropic magnetoresistance $\Delta\rho/\rho$ must then be positive as is appropriate to paraproducts of an antiferromagnetic type. The following argument resolves this contradiction.

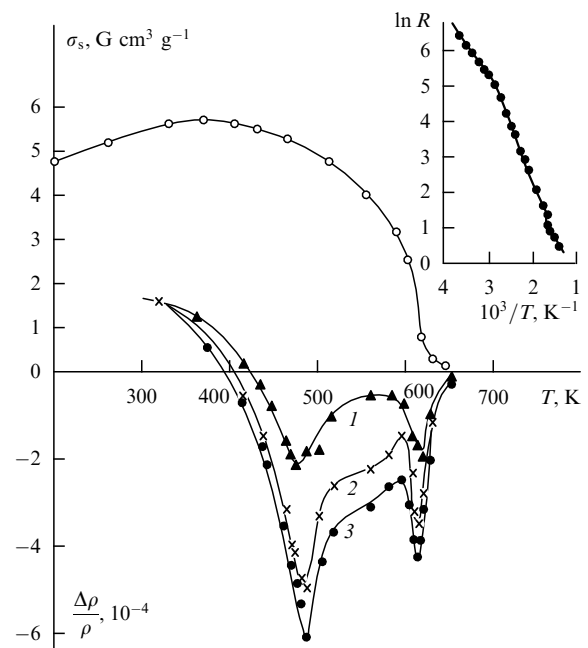


Figure 18. Temperature dependences of the spontaneous magnetization σ_s and isotropic magnetoresistance $\Delta\rho/\rho$ at $H = 6620$ (1); (2) 1650; 1230 Oe (3). Insert: the temperature dependence of the electrical resistance $\ln R(1/T)$ for the $\text{Li}_{0.5}\text{Fe}_{1.7}\text{Al}_{0.8}\text{O}_4$ ferrite.

The present author [53] has shown that hopping conduction ferrites have two isotropic magnetoresistance components. One is due to the hopping electrons being scattered off the magnetic order modified by the application of the field H (paraproduct-induced scattering). This component may have either signs, depending on whether a ferro- or antiferromagnetic paraproduct takes place. The second component is due to the hopping electrons being delocalized upon application of H . This component of isotropic magnetoresistance always

has a negative sign and, as shown in Ref. [53], is of much larger magnitude than the first.

Clearly, the situation is similar in the ferrite involved; the maximum of the positive isotropic magnetoresistance that occurs at T_B is completely overlapped with the large second component of the negative isotropic magnetoresistance. However, the relationship between the magnitudes of the first and second components is violated (in the favour of the first) as one goes away from T_B . In Fig. 18, this occurs in the range 300–400 K, where the first positive component corresponding to the antiferromagnetic paraprocess comes into play.

Thus, the low-temperature T_B point is not a feature unique to ferrimagnets with magnetic compensation points (see Table 1) but also occurs in ferrimagnets possessing anomalous temperature dependence of spontaneous magnetization (M - and P -type curves).

5. ‘Weak’ sublattice in magnetite.

On the low-temperature transformation problem ($T_t = 100$ – 120 K)

Magnetite (Fe_3O_4) belongs to a family of spinel ferrites and has been studied for over 100 years now, with particular emphasis on the so-called low-temperature transformation at $T_t = 100$ – 120 K. According to Verwey [54], this is a structural transformation caused by the ordering of iron cations of different valency (Fe^{3+} and Fe^{2+} in spinel lattice octahedra), the ordering process involving electron hopping between the cations. In the literature, therefore, this phase transition is sometimes referred to as the structural-electronic transformation, and the temperature T_t is often called the Verwey point and denoted T_V . The occurrence of dramatic variations in the magnetite cation subsystem at T_V is believed to be experimentally proved by such facts as the change in the electrical conductivity and optical absorption (due to a variation in the density and mobility of the hopping electrons), small modifications in the symmetry and parameters of the crystal lattice, etc.

There is experimental evidence, however, that certain magnetite characteristics undergo changes over the transition area $T_t = 100$ – 120 K; these include the saturation [55] and spontaneous [56] magnetization variations, appearance of the paraprocess susceptibility maximum [56] and accompanying maxima of the magnetocaloric [58, 59] and isotropic magnetoresistance [57] effects (of anomalous sign). Near T_t the changes are also observed in magnetic anisotropy [60] and other effects characteristic of magnetically ordered substances. This implies that the low-temperature transformation in magnetite is not a structural (or ‘structural-electronic’) transformation but rather a magnetic transition of some ‘special’ kind. Thus there exist at present two views in the literature on the nature of the low-temperature transformation in magnetite.

The second view will be discussed in somewhat more detail below. In a previous paper by the present author [61] it was suggested that this is a ‘magneto-electronic’ transition.

The basic idea is that beyond T_t the spin magnetic moments of the hopping electrons (whose density is very high in magnetite) become ordered and create a third — magneto-electronic — sublattice in response to the negative exchange field induced by the iron cations of the ‘combined’ BA sublattice (negative sd exchange). Since this third sublattice has its magnetic moment antiparallel to that of the

‘combined’ sublattice, this leads to some (not large) decrease in the spontaneous magnetization of the magnetite for $T < T_t$. However, at $T = T_t$ the thermal motion destroys the magnetization of the electron sublattice — partially, because at $T > T_t$ the above-mentioned negative exchange field persists — which results in a small experimentally detected I_s increase [55, 56]. The ‘magneto-electronic’ sublattice model is also capable of explaining some other effects manifested in the T_t region, for example, sign anomalies in the magnetocaloric effect and the first component of isotropic magnetoresistance, due to the antiferromagnetic-type paraprocess. Notice that Verwey’s structural-electronic model fails to account for these phenomena.

The ‘magneto-electronic’ sublattice model proposed in Ref. [61] for interpreting magnetic effects has been verified experimentally and is quite effective. However, based on the results reported in Section 4 of the present review, it can be refined somewhat in the light of a ‘weak’ sublattice concept. In magnetite, it is the ‘magneto-electronic’ sublattice which acts as ‘weak’. Referring to Fig. 19, the temperature dependence of the specific spontaneous magnetization, $\sigma_s(T)$, obtained in Ref. [56], is P -like in appearance (the departure below T_t needs verification).

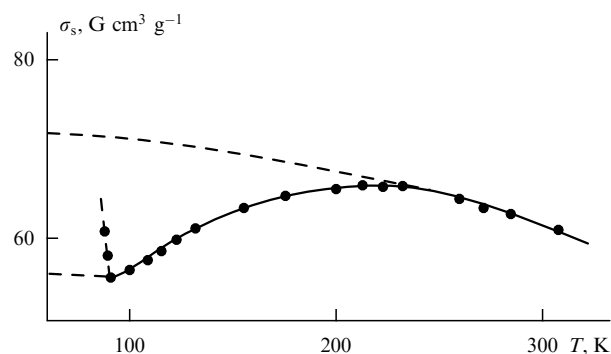


Figure 19. The temperature dependence of the magnetite specific spontaneous magnetization σ_s near the low-temperature transformation point T_t .

The above discussion suggests that T_t in magnetite is nothing but the ‘low-temperature point’ T_B of the ‘magneto-electronic’ sublattice. Application of the field H gives rise to the antiferromagnetic-type paraprocess at this point with accompanying anomalous signs for the magnetocaloric effect and the first component of the isotropic magnetoresistance, anomalies which are experimentally surveyed in magnetite near T_t . Notice that since the transition at T_B is, in a sense, a ‘retarded’ magnetic order–disorder transition (the retardation being due to the ‘strong’-sublattice-induced H_{ex} field acting continuously on a ‘weak’ sublattice), clearly the low-temperature magnetite transformation must be ‘washed out’ over a certain temperature interval, as indeed was detected experimentally.

The temperature region, in which a ‘weak’ (‘magneto-electronic’) sublattice is important, is shown schematically (to approximate scale) in Fig. 20 and it appears very small. In spite of the extensive literature on magnetite, reliable information on the temperature behaviour of I_s in this region is lacking, and it is precisely this type of data which are highly desirable to be able to prove more convincingly the present author’s hypothesis concerning the magnetic nature of the transformation at T_t .

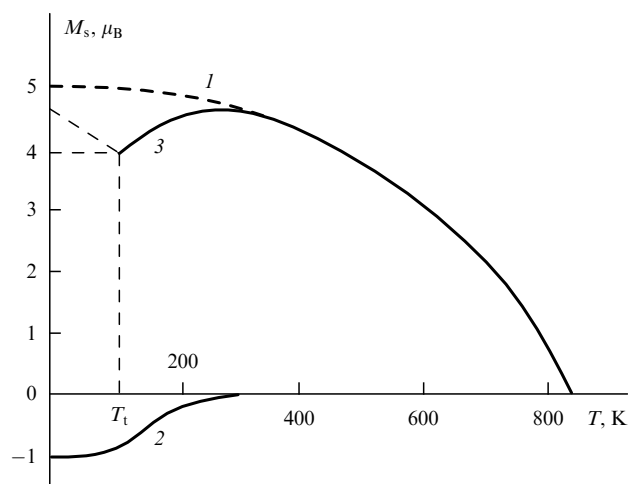


Figure 20. Schematic representation of the magnetite $I_s(T)$ dependence in the low-temperature region (to approximate scale): 1 — at $T > T_t$, 2 — for 'magneto-electronic' sublattice, 3 — at $T < T_t$.

Notice also that since the 'magneto-electronic' sublattice is 'weak' (the magnetic order of its hopping electrons is due to a moderately strong sd exchange), and because these electrons possess a greater mobility than the iron cations, this sublattice has low stability. Possible displacements of the hopping electrons (electron diffusion) in this sublattice must lead to magnetic and nonmagnetic relaxation effects in magnetite, which are especially large near T_t (as was indeed observed in the experiments).

To conclude this section we note that important evidence in favour of Verwey's hypothesis is provided by the Mössbauer [62–64] and NMR [65, 66] spectroscopy hyperfine field measurements on Fe^{2+} and Fe^{3+} cation nuclei in magnetite. At $T > T_t$, the octahedra-located Fe^{3+} and Fe^{2+} cations showed the same H_{HF} (different from the H_{HF} for the Fe^{3+} cations in tetrahedra). This means that Fe^{3+} and Fe^{2+} are indistinguishable in terms of their electronic structure at $T > T_t$. Such a situation may occur if there is intensive electron hopping between them. At $T < T_t$, the Mössbauer and NMR spectra of the octahedral Fe^{2+} and Fe^{3+} cations display two groups of resonance lines, indicating that two different values of H_{HF} , one for Fe^{2+} and the other for Fe^{3+} , exist. This is interpreted in terms of Verwey's theory in the sense that at $T < T_t$ the electrons stop hopping because of being localized on cations as a result of cation ordering.

However, the hyperfine field measurements may serve to support the 'magneto-electronic' sublattice model in magnetite, specifically at $T < T_t$, where the negative exchange field H_{ex} due to the iron cations makes the hopping electrons magnetically ordered while at the same time localizing them on these cations, and therefore different values of H_{HF} are observed on the Fe^{2+} and Fe^{3+} cations.

At $T > T_t$, where the magnetic order is partially destroyed, hopping electrons delocalize and start an intensive migration between Fe^{2+} and Fe^{3+} , creating an averaged H_{HF} field (in experiment, one value of H_{HF} is observed).

6. Conclusions

We have summarized and analyzed experimental data on the temperature dependence of spontaneous magnetization I_s of ferrimagnets with a magnetic compensation point (Néel's N

curves), and data on the anomalous temperature dependence of this magnetization in the low-temperature region (M - and P -type curves).

1. It is shown that the notion of the existence of a 'weak' sublattice in such ferrimagnets, introduced in Refs [2, 3], not only accounts for anomalous $I_s(T)$ dependences (N , M , P curves), but also explains the existence of the intensive low-temperature paraprocess of the ferro- and antiferromagnetic type in these materials. This paraprocess manifests itself in ferrimagnets with M - and P -type $I_s(T)$ dependences and, in a narrow temperature interval near the magnetic compensation point, also in those with N -type $I_s(T)$ dependences. The antiferromagnetic-type paraprocess permits the explanation of the sign anomalies which these ferrimagnets display in the magnetocaloric effect, paraprocess magnetostriction, and isotropic magnetoresistance.

2. Since the effective exchange field acting on a 'weak' sublattice from the 'strong' (Fe or Co) one is not large, the thermal motion causes a partial but very sharp magnetic disorder in the 'weak' sublattice in ferrimagnets under study, which is the origin of the so-called 'low-temperature point' T_B . The existence of the T_B point in ferrimagnets with a magnetic compensation point was predicted in 1961 [2, 3] and found experimentally in iron garnets of heavy rare-earth metals, in some rare-earth intermetallides, etc. (see Table 1). Later on, T_B points were also found in ferrimagnets with M - and P -type $I_s(T)$ dependences. The T_B point of a 'weak' sublattice is not an analogue of the Curie point T_C ; the magnetic order–disorder phase transition shows specific features at the T_B point.

3. A refinement has been introduced into the present author's [55] 'magneto-electronic' sublattice model for anomalous phenomena in magnetite (Fe_3O_4) over the area of low-temperature transformation $T_t = 100–120$ K. The 'magneto-electronic' sublattice is shown to possess the properties of a 'weak' magnetic sublattice in a ferrimagnet with an $I_s(T)$ dependence of the Néel's P type. This causes in a magnetite a low-temperature antiferromagnetic-type paraprocess accompanied by sign anomalies in the magnetocaloric effect and in the first component of the isotropic magnetoresistance. The magnetite low-temperature T_B point is none other than the low-temperature transformation temperature T_t .

Thus, identifying the 'magneto-electronic' sublattice with a 'weak' sublattice provides a good understanding of the 80-years-old problem of the transformation nature at the T_t point.

References

1. Néel L *Ann. Phys. (Paris)* **3** 137 (1948)
2. Belov K P *Zh. Eksp. Teor. Fiz.* **41** 692 (1961) [*Sov. Phys. JETP* **14** 499 (1962)]
3. Belov K P *Izv. Akad. Nauk SSSR Ser. Fiz.* **25** (11) 1320 (1961)
4. Belov K P *Ferrity v Sil'nykh Magnitnykh Polyakh* (Ferrites in Strong Magnetic Fields) (Moscow: Nauka, 1972)
5. Pauthenet R *Ann. Phys. (Paris)* **29** 253 (1958)
6. Ped'ko A V *Zh. Eksp. Teor. Fiz.* **41** 700 (1961) [*Sov. Phys. JETP* **14** 505 (1962)]
7. Belov K P, Sokolov V I *Izv. Akad. Nauk SSSR Ser. Fiz.* **30** (6) 1073 (1966) [*Bull. Acad. Sci. USSR Phys. Ser.* **30** 1120 (1966)]
8. Buschow K H J *Phys. Status Solidi* **7** 199 (1971)
9. Belov K P et al. *Zh. Eksp. Teor. Fiz.* **64** 2154 (1973) [*Sov. Phys. JETP* **37** 1086 (1973)]
10. Belov K P et al. *Fiz. Met. Metalloved.* **34** 470 (1972)
11. Ermolenko A S et al. *Zh. Eksp. Teor. Fiz.* **69** 1743 (1975) [*Sov. Phys. JETP* **42** 885 (1975)]

12. Berezin A G, Levitin R Z, Popov Yu F *Zh. Eksp. Teor. Fiz.* **79** 268 (1980) [*Sov. Phys. JETP* **52** 135 (1980)]
13. Hasegawa R et al. *AIP Conf. Proc.* **24** 110 (1975)
14. Gorter E W, Schulkes J A *Phys. Rev.* **90** 487 (1953)
15. Goryaga A N, Lin' Chzhan-ta *Zh. Eksp. Teor. Fiz.* **41** 696 (1961) [*Sov. Phys. JETP* **14** 502 (1962)]
16. Belov K P, Goryaga A N, Gridasova T Ya *Fiz. Tverd. Tela* (Leningrad) **14** 1428 (1972) [*Sov. Phys. Solid State* **14** 1225 (1972)]
17. Novogrudskii V N, Fakidov I G *Zh. Eksp. Teor. Fiz.* **59** 1983 (1970) [*Sov. Phys. JETP* **32** 1074 (1971)]
18. Yasukochi K, Kanematsu K, Ohoyama T *J. Phys. Soc. Jpn.* **15** 932 (1960)
19. McGuire T R, Greenwald S W *Sol. St. Phys. Electr. Telecom.* **58** 515 (1970)
20. Nikolaev V I, Popov F I, Cherepanov V M *Zh. Eksp. Teor. Fiz.* **58** 515 (1970) [*Sov. Phys. JETP* **31** 276 (1970)]
21. Belov K P, Shlyakhina L P, in *Fizika i Khimiya Ferritov* (Physics and Chemistry of Ferrites) (Moscow: Moscow State University, 1973) p. 116
22. Pauthenet R *J. Ann. Phys. (Paris)* **3** 424 (1958)
23. Aleonard R J. *Phys. Chem. Solids* **15** 167 (1960)
24. Anderson P W *Sol. St. Phys.* **14** 99 (1966)
25. Meyers S M et al. *Phys. Rev.* **170** 533 (1968)
26. Atzmony U, Mualem A, Ofer S *Phys. Rev.* **136** B1237 (1964)
27. Belov K P, Nikitin S A *Phys. Status Solidi* **12** 453 (1965)
28. Belov K P et al. *Zh. Eksp. Teor. Fiz.* **61** 1101 (1972) [*Sov. Phys. JETP* **34** 588 (1972)]
29. Kamilov I K, Aliev Kh K *Staticheskie i Kriticheskie Yavleniya v Magnitouporyadochennykh Kristallakh* (Static and Critical Phenomena in Magnetically Ordered Crystals) (Makhachkala: Dagestan Branch of the Russian Acad. of Sci., 1993)
30. Belov K P et al. *Pis'ma Zh. Eksp. Teor. Fiz.* **9** 671 (1969) [*JETP Lett.* **9** 416 (1969)]
31. Belov K P et al. *Zh. Eksp. Teor. Fiz.* **62** 2183 (1972) [*Sov. Phys. JETP* **35** 1142 (1972)]
32. Andreenko A S et al. *Usp. Fiz. Nauk* **158** 553 (1989) [*Sov. Phys. Usp.* **32** 649 (1989)]
33. Belov K P et al. *Zh. Eksp. Teor. Fiz.* **38** 1908 (1960) [*Sov. Phys. JETP* **11** 1372 (1960)]
34. Belov K P et al. *Zh. Eksp. Teor. Fiz.* **40** 752 (1961) [*Sov. Phys. JETP* **13** 527 (1961)]
35. Belov K P et al. *Fiz. Tverd. Tela* (Leningrad) **11** 191 (1969)
36. Belov K P *Vestn. Mosk. Univ. Ser. Fiz. Astron.* **34** 6 (1993)
37. Belov K P et al. *Pis'ma Zh. Eksp. Teor. Fiz.* **10** 13 (1969) [*JETP Lett.* **10** 8 (1969)]
38. Belov K P, Levitin R Z, Popov Yu F *Zh. Eksp. Teor. Fiz.* **59** 1985 (1970) [*Sov. Phys. JETP* **32** 1076 (1971)]
39. Novogrudskii V N, Fakidov I G *Zh. Eksp. Teor. Fiz.* **47** 40 (1964) [*Sov. Phys. JETP* **20** 28 (1965)]
40. Vlasov K B et al., in *Dinamicheskie i Kineticheskie Svoïstva Magnetikov* (Dynamical and Kinetic Properties of Magnetic Materials) (Moscow: Nauka, 1986) p. 37
41. Turov E A, Shavrov V G *Zh. Eksp. Teor. Fiz.* **43** 2273 (1962) [*Sov. Phys. JETP* **16** 1606 (1963)]
42. Clark A E, Callen E J. *Appl. Phys.* **39** 5972 (1968)
43. Belov K P et al. *Orientatsionnye Perekhody v Redkozemel'nykh Magnetikakh* (Orientational Transitions in Rare-Earth Magnetic Materials) (Moscow: Nauka, 1979)
44. Zvezdin A K, Matveev V M *Zh. Eksp. Teor. Fiz.* **62** 260 (1972) [*Sov. Phys. JETP* **35** 140 (1972)]
45. Kudrevatykh N V Author's Abstract of Doctor's Dissertation (Ekaterinburg: Ural State University, 1994)
46. Druzhinin V V, Zapasskii S P, Povyshev V M *Fiz. Tverd. Tela* (Leningrad) **19** 159 (1977) [*Sov. Phys. Solid State* **19** 90 (1977)]
47. Belov K P, Malevskaya L A *Izv. Akad. Nauk SSSR Ser. Fiz.* **25** 1371 (1961)
48. Goryaga A N, Gridasova T Ya, in *Ferrimagnetizm* (Ferrimagnetism) (Moscow: Moscow State University, 1975) p. 124
49. Belov K P et al. *Pis'ma Zh. Eksp. Teor. Fiz.* **16** 448 (1972) [*JETP Lett.* **16** 317 (1972)]
50. Belov K P, Goryaga A N, Kokorev A I *Fiz. Tverd. Tela* (Leningrad) **28** 1588 (1986) [*Sov. Phys. Solid State* **28** 901 (1986)]
51. Belov K P et al. *Fiz. Tverd. Tela* (Leningrad) **16** 295 (1974) [*Sov. Phys. Solid State* **16** 199 (1974)]
52. Belov K P, Goryaga A N, Gridasova T Ya *Fiz. Tverd. Tela* (Leningrad) **12** 277 (1970)
53. Belov K P *Usp. Fiz. Nauk* **164** 603 (1994) [*Phys. Usp.* **37** 563 (1994)]
54. Verwey E J W *Nature* (London) **144** 327 (1939)
55. Weiss P, Forrer R *Ann. Phys. (Paris)* **12** 279 (1929)
56. Skipetrova L A Thesis for Candidate's Degree (Moscow: Moscow State University, 1978)
57. Halileev P A *Sov. Phys.* **7** 108 (1935)
58. Krasovskii V P, Fakidov I G *Zh. Eksp. Teor. Fiz.* **39** 235 (1960) [*Sov. Phys. JETP* **12** 170 (1961)]
59. Belov K P et al. *Pis'ma Zh. Eksp. Teor. Fiz.* **36** 118 (1982) [*JETP Lett.* **36** 146 (1982)]
60. Abe K, Miyamoto Y, Shikazumi S *J. Phys. Soc. Jpn.* **41** 1894 (1976)
61. Belov K P *Usp. Fiz. Nauk* **163** (5) 53 (1993) [*Phys. Usp.* **36** 380 (1993)]
62. Bauminger R et al. *Phys. Rev.* **122** 1447 (1961)
63. Ito A, Ono K, Ishikawa Y *J. Phys. Soc. Jpn.* **18** 1465 (1963)
64. Romanov V P, Checherskii V D, Eremenko V V *Phys. Status Solidi* **31** K153 (1969)
65. Kovtun N M, Solov'ev E E, Shemyakov A A *Fiz. Tverd. Tela* (Leningrad) **14** 2799 (1972) [*Sov. Phys. Solid State* **14** 2430 (1973)]
66. Kovtun N M, Shemyakov A A *Fiz. Tverd. Tela* (Leningrad) **15** 1625 (1973) [*Sov. Phys. Solid State* **15** 1625 (1973)]